Article type (Article)

iEnergy

# Optimal Urban EV Charging Station Site Selection and Capacity Determination Considering Comprehensive Benefits of Vehicle-Stations-Grid

Hongwei Li[1], Yufeng Song[1], Jiuding Tan[2], Yi Cui[3], Shuaibing Li[2,*], Yongqiang Kang[2], Haiying Dong[2]

1 School of Automation and Electrical Engineering, Lanzhou Jiaotong University, Lanzhou, 730070, China
2 School of New Energy and Power Engineering, Lanzhou Jiaotong University, Lanzhou, 730070, China
3 School of Engineering, University of Southern Queensland, Springfield 4300, Australia
*Corresponding author Shuaibing Li; shuaibingli@mail.lzjtu.cn

## ABSTRACT

The proposal introduced an urban electric vehicle (EV) charging station location and capacity optimization model that considers the comprehensive interests of the "vehicle-station-network" system. This method employs ArcScene for the coupling of road-electric models and aims to minimize the total societal cost, composed of the charging station operator's cost, the user's charging cost, and the electric grid's loss cost, as the objective function. It solves the problem using an immune particle swarm optimization (PSO) algorithm that combines PSO with the immune algorithm. The model is then applied to simulate the charging station location and sizing issues within the study area. The simulation results demonstrate that the proposed immune particle swarm optimization algorithm (IPSOA) has good convergence and is more advantageous in solving multimodal functions. Meanwhile, the method takes into account the interests of charging station users, operators, and the electric grid, resulting in a decrease of electrical grid loss cost by 11.1% and 17.8%, and a reduction of the total societal cost by 9.96% and 3.22%, respectively, compared to two other location schemes.

## KEYWORDS

Electric vehicles; charging station; site selection and capacity determination; ArcScene; immune particle swarm optimization algorithm; road electrical coupling



## 1 Introduction

Currently, the international energy crisis is intensifying, and environmental pollution issues have become more pronounced. Traditional fuel-powered vehicles with high energy consumption and pollution levels are no longer suited to the future development direction. Efficient and low-carbon EVs have received significant attention from governments worldwide and have become key to breaking the energy crisis and solving environmental issues. Advancing the EV industry relies on the construction of supporting facilities such as charging stations. However, the current planning and design of EV charging stations have not been scientifically rationalized, leading to low utilization rates of charging facilities, poor economic benefits for operators, and difficulties for users in charging their vehicles. Therefore, research into the location and capacity determination of EV charging stations is necessary. Location and sizing are influenced by numerous factors. First, there is strong randomness in the spatial and temporal distribution of EV charging loads, making accurate prediction of charging demand challenging. Secondly, location and sizing of charging stations belong to a multi-objective planning issue that needs to address the fair distribution of interests among operators, users, and the electric grid to ensure safety, economy, and convenience of the solution. As a result, different scholars have variable planning objectives when conducting related research, which has led to a diversity of models for the location and sizing of EV charging stations. Currently, the more commonly used models can be divided into three categories: P-Median models, P-Center models, and Flow Covering Location Models (FCLM).

The P-Median model is often used in situations where the maximum budget for building stations is given and the number of stations to be built within a region is fixed. This model begins by selecting charging demand points within the study area, and then establishes weighted distance connections between the charging demand points and the potential charging station locations, searching for the solution where the sum of weighted distances from all charging demand points to the charging station is minimized. Y. Feng et al. [1] used an improved K-means clustering algorithm

to analyze the distribution characteristics of urban EV charging demand points. After a given number of stations is determined, it solves for the optimal siting and capacity plan under different numbers of charging stations with the objective of minimizing the distance from each charging demand point to the planned charging stations.

P-Center is similar to P-Median, but its planning objective is to minimize the maximum distance from any charging demand point to the nearest charging station. L. Jia et al. [2] improved upon the P-Center model by considering the charging patterns of EVs under different charging demands and modeling the road network structure to analyze the impact of traffic flow on the site and capacity planning of charging stations. The optimization objective is to minimize the comprehensive cost while ensuring the safe operation of the electric grid, ultimately determining the optimal location for charging stations. S. Ge et al. [3] took into account the interests of both EV users and charging station operators, using the total societal cost as the objective function. It weights the factors affecting siting of EV charging stations and uses a Voronoi diagram to divide the service range of the charging stations, enhancing the convenience of charging for EV users. W. Huang et al. [4-5] focused on the difference in charging needs of EV users, quantifying users' travel and charging patterns, using the Monte Carlo method to simulate the spatio-temporal distribution of charging demand within the study area, and likewise using a Voronoi diagram to divide the service range of the charging stations.

The central idea of FCLM is that charging stations, while meeting all the EV charging needs in the study area, should reduce the comprehensive cost of construction, i.e., meet as many charging demands as possible with fewer stations and lower budget costs. Q. Xu et al. [6] aimed to improve the service quality and rate of EV charging stations, characterizing user behavior habits based on the travel chain model, and expanding the coverage of charging stations based on the Voronoi diagram concept as much as possible while meeting user charging needs [7]. F. Wu et al. [8] proposed a stochastic truncated coverage model to optimize the siting and capacity of a limited number of fast charging stations for EVs within a given study area. The method analyzes through a two-stage stochastic integer program, the first stage determines the locations to build stations, and the second stage determines the flow of EVs. The method is applied to a case study in Ohio, showing that the same number of EVs charging stations can meet more charging demands, i.e., capture more EV flow within the area. M. Kchaou-Boujelben et al. [9] based on the randomness of vehicle driving range and mileage, consider the variability of traffic conditions in different areas and the correlation with corresponding random power consumption, proposing an opportunity-constrained truncation model. In this model, if the coverage rate of traffic flow remains above a pre-set minimum value, then the flow is considered to be covered. O. Arslan et al. [10] took into account not only pure EVs when siting charging stations but also plug-in hybrid EVs and multiple EV models with different ranges, which more closely corresponds to the actual situation where pure EVs and hybrid vehicles coexist, having greater practical significance. C. Lee et al. [11] believed that a vehicle's maximum driving distance may vary based on environmental factors, such as traffic conditions, weather, temperature, etc. Therefore, it proposes to integrate a probability reachability function into the existing probabilistic expansion network method to analyze, abstracting the siting problem as a mixed-integer nonlinear programming problem and using this method to conduct a verification simulation for a segment of highway in Texas. The method not only has advantages in computation time but also produces better solutions under the assumption of uncertain travel ranges. J. Hondgsonm et al. [12] proposed an FCLM based on road network flow demand for charging facilities, i.e., to build a given number of charging facilities under the condition of a given traffic road network and flow to maximize the captured traffic flow. H. Wang et al. [13] considered the dual attributes of public service and common power usage of EV charging stations, constructing an optimization model for siting charging stations that can capture the maximum traffic flow and meet the minimum power grid loss. The model uses a gravity spatial interaction calculation for traffic flow and a super-efficiency data envelopment analysis method to decompose the multi-objective decision problem into single-objective optimization for solution. Building on H. Wang et al. [13], W. Yao et al. [14] also considered the investment costs of charging station operators, sets maximum thresholds for the waiting time of EV users during peak travel periods, and introduces a traffic assignment model based on user equilibrium to calculate the traffic flow captured by the charging stations. X. Huang et al. [15] focused on the operational costs of the charging station investors, proposing a quantum genetic algorithm for charging station siting. This algorithm uses FCLM to constrain the location of charging stations and traffic flow, with the goal of maximizing economic benefits for investors, providing theoretical guidance for the current work of EV charging station siting.

From the above, it is clear that current mainstream models for optimizing the location of charging stations, such as the P-Median, P-Center, and FCLM, still cannot adequately accommodate all the factors influencing the decision-making process for the location and capacity optimization. Research by scholars both domestically and internationally has mostly focused on the investment returns for charging station investors, capturing traffic flow in road networks, and the cost of electrical grid losses. They have not comprehensively considered the multi-objective layout optimization problems under the multi-source information fusion mode of "vehicle-road-electricity" Therefore, this paper proposes a multi-source information fusion model for the location and capacity determination of EV charging stations, which achieves a rational layout design for EV charging stations and has significant theoretical value and practical

significance for multi-objective planning of EV charging stations.

The main contributions of this paper are as follows:

(1) Considering the optimal benefit distribution under the vehicle-station-network model, objective functions and constraint equations for the vehicle, the charging station, and the grid are established respectively.

(2) A network-grid coupling method based on ArcScene is proposed, which enhances the applicability of the model.

(3) An IPSOA, which combines the PSO algorithm with the immune algorithm (IA), is used for solving, improving the precision of the solutions.

The main body of the paper is organized as follows: Section one briefly introduces the three main entities of the multi-source information fusion framework and their interactions. Section two constructs the road network-electric grid coupling model based on ArcScene. Section three constructs the objective functions and constraint functions for the location and sizing of charging stations. Section six proposes the IPSOA and conducts algorithm testing, building upon the PSO and Immune algorithms introduced in sections four and five. Section seven verifies the effectiveness of the proposed method through simulation examples. Finally, section five concludes the paper.

## 2 Multi-source information fusion framework

Previous planning models for charging stations often assumed that information such as the electric grid and road network is static, without considering the dynamic changes and interactions of information. This paper proposes an EV charging station planning model based on the multi-source information fusion of vehicles, roads, and electricity. As illustrated in Figure 1, the multi-source information fusion framework includes three main entities: vehicles, road networks, and electric grids.

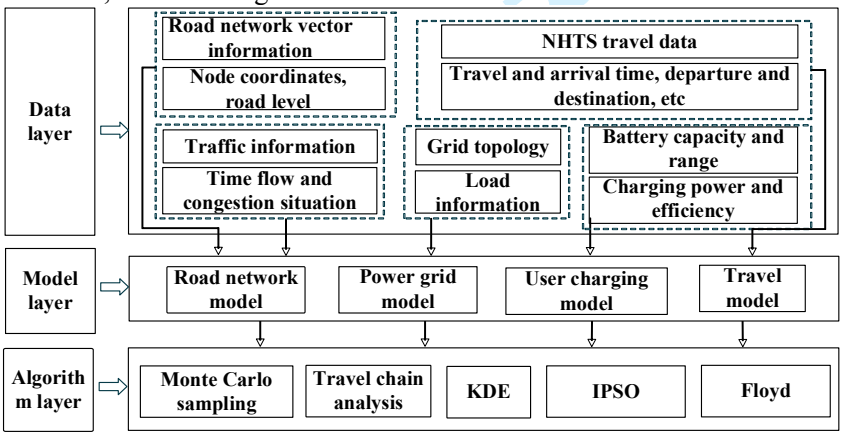


**Fig. 1. Relationship framework of multi-source information fusion data layer, model layer, and algorithm layer**

(1) Vehicle: This encompasses various aspects such as vehicle driving characteristics, EV charging behavior, and battery performance parameters. EV driving characteristics include departure times, points of origin and destination, and choices of driving routes. During a trip, the driver determines the shortest route using the Floyd algorithm.

(2) Road Network: This involves the location of traffic nodes, spatial distribution of different urban functional areas, road network structure, traffic congestion, and real-time driving speeds of vehicles. Using ArcGIS to build the road network model, land attributes of different functional areas are classified, generally divided into office areas, residential areas, commercial areas, and public service areas. Additionally, the level of traffic congestion not only reflects the information on road traffic flow and speed but also can influence drivers' route selection preferences to some extent.

(3) Electric Grid: This includes the distribution network structure, power supply node loads, and EV charging pricing. In the distribution network, charging pricing is one of the key factors that users consider when choosing the location of charging facilities. A large non-uniform integration of the EV charging load could lead to voltage collapse issues. Therefore, developing a reasonable electric grid model is especially important.

# 3 A road network and power grid coupling model based on ArcScene

## 3.1 Distribution network model

To study the impact of EVs on the grid, a model must be developed that matches the road network in the study area. The basic load and charging load in the area are allocated to the corresponding nodes, neglecting the presence of switches in the grid and simplifying the grid into a combination of nodes and lines. The distribution system is modeled using a four-tuple:

$$P = \left\{ N_G, L_G, B_G, S_G \right\} \tag{1}$$

$$N_G = \left\{ (1, n_1), (2, n_2), \mathrm{L}\ (g, n_g) \right\} \tag{2}$$

where $N_G$ is the set of nodes, indicating the node number and node type. When $n_i$=1, it is a $PQ$ node, which corresponds to a load connected to the distribution network. When $n_i$=2, it is a voltage magnitude and phase angle specified node, equivalent to a transformer in the distribution network that is directly connected to a higher voltage level.

$$L_G = \left\{ (n_i, n_j) \,|\, 1 \le i, j \le \mathrm{g} \right\} \tag{3}$$

where $L_G$ is the set of branches, representing each line's starting and ending nodes.

$$B_G = \left\{ (R_k + jX_k) \,|\, 1 \le k \le 1 \right\} \tag{4}$$

where $B_G$ stands for the set of branch impedances, representing the resistance and reactance of each branch in the distribution network.

$$S_G = \left\{ (P_k + jQ_k) \,|\, 1 \le k \le \mathrm{g} \right\} \tag{5}$$

where $S_G$ is the set of nodal power, indicating the load size carried by each node in the power grid.

## 3.2 Coupling of road network and power grid

Combining the road network model and the power grid model, ArcScene is used to couple the two networks. ArcScene is a three-dimensional geographic information system software primarily used to create, edit, analyze, and visualize three-dimensional geographic information data. It can perform functions such as data visualization, editing, spatial analysis, data import and export, and geospatial simulation [16] The steps for the road network-electric grid coupling are as follows: First, a point feature layer is established by converting road and electric grid model node information into suitable quantitative matrices and importing them into ArcScene to create a node layer. Second, a face feature layer is established by importing the road and electric grid model node adjacency matrices, creating the road and electric grid face structure layers. Finally, the road network node matrix corresponding to the electric grid nodes is set, and the height of the electric grid layer is adjusted to generate a three-dimensional coupled road network-electric grid map. As shown in Figure 2, this presents a coupling effect diagram within the study area's road network model and the IEEE 33-node system.

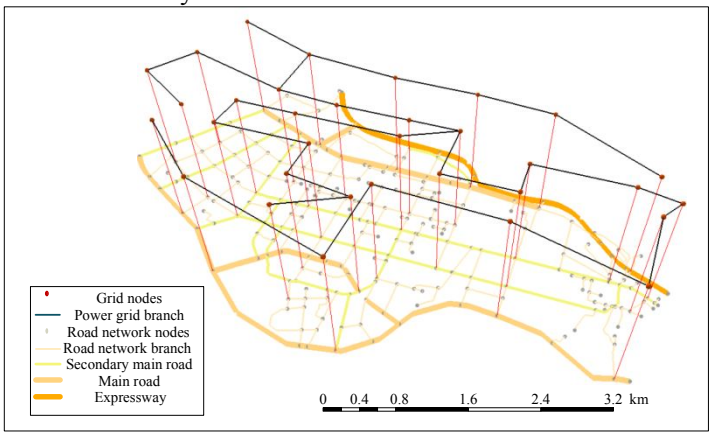


**Fig. 2. Three dimensional results of road network power grid coupling based on ArcScene**

# 4 Coupled road-network grid model based on ArcScene

## 4.1 Objective function

The location and sizing model for EV charging stations takes into account the costs of EV charging station operators, the charging costs for EV users, and the cost of losses in the electric grid. The overall goal is to minimize the total cost to society, with the total target function as shown in Eq. (6).

$$C_{\min} = C_{\text{op}} + C_{\text{u}} + C_{\text{p}} \tag{6}$$

where $C_{\text{op}}$ is the cost for EV charging station operators, $C_{\text{u}}$ is the charging cost for EV users, and $C_{\text{p}}$ is the cost of losses in the electric grid.

(1) EV Charging Station Operator Costs

The cost for EV charging station operators consists of two parts: the construction and the operation & maintenance costs. This can be represented as:

$$C_{\text{op}} = C_{\text{opc}} + C_{\text{opr}} \tag{7}$$

where $C_{\text{opc}}$ is the construction cost for charging station operators, and $C_{\text{opr}}$ is the operation & maintenance cost for charging station operators.

1) Construction Cost for Charging Station Operators

The construction cost for charging station operators considers the building expenses incurred over the operational lifespan of the charging piles. This includes hardware costs such as the purchase and installation of charging piles and transformers, as well as costs for preliminary investigations, scheme development, environmental protection, and site construction. It is represented by:

$$C_{\text{opc}} = \sum_{i=1}^{N} \left( C_{\text{opcb}} + n_i C_{\text{opcp}} + \frac{r_0 (1+r_0)^m}{(1+r_0)^m - 1} b_i C_{\text{opce}} + \alpha n_i C_{\text{r}} \right) \tag{8}$$

where $N$ is the total number of charging stations, $i$ is the identifier for the charging station, $n_i$ is the total number of charging piles in the $i$-th charging station, $\alpha$ is the construction floor area related to each charging pile, $b_i$ is the number of transformers in the $i$-th charging station, $m$ is the service life of the charging station, $C_{\text{r}}$ is the annual rent per unit area of the charging station, $r_0$ is the rate of return on investment, $C_{\text{opcb}}$ is the fixed construction cost for the charging station, $C_{\text{opcp}}$ is the cost of purchase and installation for each charging pile, $C_{\text{opce}}$ is the cost of purchase and installation for each transformer.

2) Operation & Maintenance Cost for Charging Station Operators

Charging station operators need to pay annual operation and maintenance costs, which include the cost of electricity during regular operation and the cost of repairs during abnormal operations. This is represented by:

$$C_{\text{opr}} = \sum_{i=1}^{N} m n_i (C_{\text{oprp}} + n_i P_{\text{ch}} t_{\text{r}} C_{\text{ep}}) \tag{9}$$

where $C_{\text{oprp}}$ is the average maintenance cost per charging pile per year, $p_{\text{ch}}$ is the average charging power per charging pile per year, $t_{\text{r}}$ is the average charging time per charging pile per year, $C_{\text{ep}}$ is the cost per unit of electricity purchased.

(2) Charging Costs for EV Users

The charging costs for EV users include not only the fees paid for using the charging piles but also the loss of cost for traveling to the charging station (the cost of electricity during this period and the equivalent economic value of time) as well as the lost time cost while queuing inside the charging station. This can be represented as:

$$C_{\text{u}} = \sum_{i=1}^{N} m (C_{\text{u1}} + C_{\text{u2}} + C_{\text{u3}}) \tag{10}$$

where $C_{\text{u1}}$ is the loss cost of traveling to the charging station for users, $C_{\text{u2}}$ is the lost cost of queuing inside the charging station for users, $C_{\text{u3}}$ is the charging cost for users.

1) Loss cost of traveling to the charging station for users

$$C_{\text{u1}} = \sum_{s=1}^{S} \left( l_0 l_{\text{is}} C_{\text{chp}} + \frac{l_{\text{is}}}{v_{\text{is}}} C_{\text{t}} \right) \tag{11}$$

where $s$ is the identifier for users waiting to charge, $S$ is the total number of users waiting to charge, $\lambda_0$ is the unit mileage electricity consumption for EVs, $l_{\text{is}}$ is the shortest distance traveled by users to the charging station, $C_{\text{chp}}$ is the charging price for users, $v_{\text{is}}$ is the average speed of users traveling to the charging station, $C_{\text{t}}$ is the economic cost per unit of time.

2) Lost time cost while queuing inside the charging station for users

The user queuing situation inside the charging station is shown in Figure 3 as a single queue model. The EV queuing state transition diagram is illustrated in Figure 4, described by the M/M/n model.

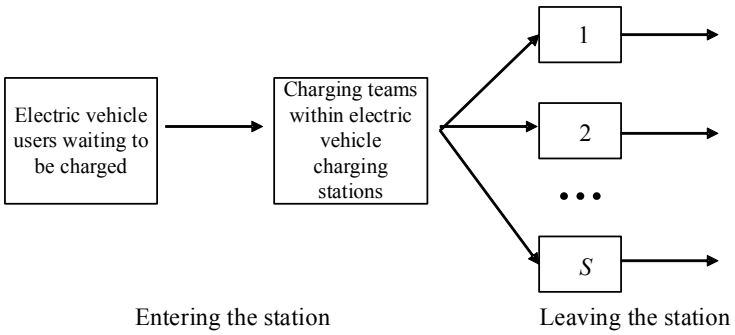


**Fig. 3. Charging station user queuing mode**

The steady-state equilibrium equation for the M/M/n queuing system is shown in formulas below, which is solved in conjunction with Eq. (12), (13), (14), and (15).

$$\begin{cases} \lambda P_0 = \mu P_1 \\ \lambda P_{f-1} + (f+1)\mu P_{f+1} = (\lambda + f\mu)P_f \\ n\mu P_{f+1} + \lambda P_{f-1} = (\lambda + n\mu)P_f \end{cases} \tag{12}$$

$$P_0 = \left[ \sum_{s=0}^{n-1} \frac{1}{s!} (\frac{\lambda}{\mu})^s + \frac{1}{n!} \frac{1}{1-\rho} (\frac{\lambda}{\mu})^n \right]^{-1} \tag{13}$$

$$P_n = \begin{cases} \frac{1}{n!} (\frac{\lambda}{\mu})^n P_0 & f \le n \\ \frac{1}{n! n^{f-n}} (\frac{\lambda}{\mu})^f P_0 & f > n \end{cases} \tag{14}$$

$$\rho_n = \lambda / (n\mu) \tag{15}$$

where $\lambda$ is the arrival rate of vehicles, $\rho$ denotes the service intensity, $\mu$ is the average service rate, $f$ is the number of EVs waiting to be charged within the charging station, $n$ is the total number of charging piles in the charging station. If $f$ is less than or equal to $n$, then the average service rate of the entire charging station is $f\mu$, if $f$ is greater than $n$, the average service rate is $n\mu$.

Therefore, the lost time cost while queuing inside the charging station for users can be represented as:

$$C_{u2} = \sum_{i=1}^{N} \sum_{t=1}^{t_r} W_q^i \lambda_t^i C_t \tag{16}$$

$$W_q^i = \frac{\rho^n}{n!(1-\rho_n)} p_0 \int_0^\infty t \mathrm{d}(-\mathrm{e}^{-(1-\rho_n)n\mu t}) \tag{17}$$

where $Wi\ q$ is the expected waiting time for EV charging within the charging station identified by $i$, $\lambda i\ t$ is the number of EVs heading towards the $i$-th charging station at time $t$.

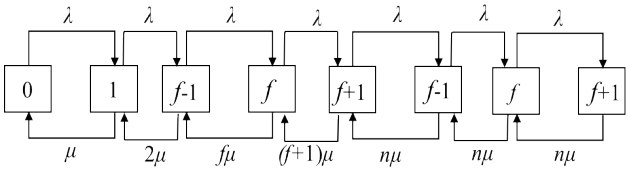


**Fig. 4. Charging station user queuing mode**

3) Charging Cost for Users

$$C_{u3} = P_{ch} t_{ch} C_{chp} \tag{18}$$

where $P_{ch}$ is the average annual charging power, $t_{ch}$ is the average annual charging time.

(3) Cost of Losses in the Electric Grid

$$C_{loss} = m P_{lossp} t_r n_i C_{lossp} \tag{19}$$

where $C_{lossp}$ is the unit loss cost for the distribution network line, $P_{lossp}$ is the loss value for the distribution network line.

## 4.2 Constraint conditions

The constraints of the EV charging station location and capacity model involve three main entities. Firstly, for the charging station operator: constraints such as the number of charging stations, service range of the charging station, distance between adjacent charging stations, and the capacity of the charging stations are considered. Secondly, for the charging customers: the main concern is constraints on the waiting time for customers queuing up to charge. Finally, for the distribution network: constraints include the upper and lower limits of node voltage magnitudes, the maximum charging power that can be integrated into the power grid, and the maximum current in feeders.

1) Constraints on the number of charging stations

$$N_{\min} \le N \le N_{\max} \tag{20}$$

where $N_{\min}$ is the minimum number of planned charging stations, $N_{\max}$ is the maximum number of planned charging stations

2) Service range constraints for charging stations

The service range of charging stations should meet the charging needs of users within the area, which can be expressed as:

$$\sum_{i=1}^{N} n_i P_{\mathrm{ch}} t_{\mathrm{r}} \ge M_{\max}(1+\varphi) \tag{21}$$

where $M_{\max}$ is the total demand for EV charging in the service area, $\varphi$ is the charging loss rate within the charging station.

3) Distance constraints between adjacent charging stations

The distance between two adjacent charging stations should be appropriate, not too far or too close, which can be expressed as:

$$l_{\mathrm{S}} \le l(N_i, N_j) \le 2l_{\mathrm{S}} \tag{22}$$

where $l_{\mathrm{S}}$ is the service radius of the charging station, $l(N_i,N_j)$ is the distance between two adjacent charging stations.

4) Power constraints for charging stations

The charging power of the charging station should be less than or equal to the maximum power allowed by the distribution network node to which it is connected.

$$P^{i}_{ch,\max} \le P^{i}_{j\max} \tag{23}$$

where $Pi\ ch$,max is the maximum charging power for charging station number $i$, P$i\ j$,max is the maximum charging power allowed by the distribution network node to which charging station number $i$ is connected.

(2) Constraints on User Queuing Waiting Time

$$W^{i}_{\mathrm{q}} \le W_{\mathrm{qmax}} \tag{24}$$

where $W_{\mathrm{qmax}}$ is the maximum waiting time of EV users waiting to be charged in the charging station.

(3) Distribution Network

1) Node voltage amplitude bound constraints

$$V_i^{\min} \le V_i \le V_i^{\max} \qquad i, j = 1,2,\mathrm{L}\ ,Q \tag{25}$$

where $V$min $i$ is the lower limit of node voltage amplitude, $V$max $i$ is the upper limit of node voltage amplitude, $Q$ is the number of nodes in the distribution network.

2) Maximum charging power constraint of the distribution network

$$\sum_{i=1}^{N} P_{\mathrm{ch},\max} + P_{\mathrm{total},\max} \le P_{\max} \tag{26}$$

where $P_{\mathrm{total,max}}$ is the maximum base power allowed to connect to the distribution network excluding the charging station power, $P_{\max}$ is the maximum power that can be admitted to the distribution network.

3) Maximum current constraint for feeders

$$\left|I_{ij}\right| \le I_{ij\max}, \quad i, j = 1,2,\mathrm{L}\ ,Q \tag{27}$$

where $I_{ij}$ represents the current passing through feeder $ij$ in the distribution network.

## 5 Principle of IPSOA algorithm

The PSO is an evolutionary computational technique developed by Kennedy and Eberhart in 1995 [17] In PSO, each search individual is abstracted as a particle without mass and volume, flying at a particular rate in the solution space. Through learning and iteration, particles adjust their flight speed based on individual and group experience. In the process of seeking the optimal solution, each particle determines its fitness according to the function value to be optimized. This information includes the current position of the particle, the best position found (i.e., individual experience), and the optimal position found in the group (i.e., group experience). Therefore, the movement of the

particles is influenced by both individual historical states and group historical states. By adjusting the current direction and speed of the particles, the particle swarm algorithm effectively coordinates the dynamic relationship between individuals and groups.

When a particle swarm is in D-dimensional space, and N particles are generated, the expression is:

$$\begin{cases} X_i^t = \left(x_{i1}^t, x_{i2}^t, \text{L}\ x_{iD}^t\right), & i = 1,2,\text{L}\ ,N \\ V_i^t = \left(v_{i1}^t, v_{i2}^t, \text{L}\ v_{iD}^t\right), & i = 1,2,\text{L}\ ,N \end{cases} \tag{28}$$

where *Xt i* is the position of the *i*-th particle at the *t*-th iteration, *Vt i* represents the velocity of the *i*-th particle at the *t*-th iteration.

$$\begin{cases} P_{i,\text{best}}^t = \left(p_{i1}^t, p_{i2}^t, \text{L}\ p_{iD}^t\right), & i = 1,2,\text{L}\ ,N \\ P_{g,\text{best}}^t = \left(p_{g1}^t, p_{g2}^t, \text{L}\ , p_{gD}^t\right) \end{cases} \tag{29}$$

where *Pt i,*best is the best value found by the *i*-th particle after the *t*-th iteration, which is the individual best solution, *Pt g,*bes*t* is the best value found by the group after the *t*-th iteration, which is the global best solution.

The formulas for iterative calculation of each particle's velocity and position are:

$$\begin{cases} v_i^{t+1} = \omega v_i^t + c_1 r_1 \left(p_{i,\text{best}}^t - x_i^t\right) \\ +c_2 r_2 \left(p_{g,\text{best}}^t - x_i^t\right) \\ x_i^{t+1} = x_i^t + v_i^{t+1} \end{cases} \tag{30}$$

where $\omega$ is the inertia weight, $c_1$ and $c_2$ are learning factors, and $r_1$ and $r_2$ are random numbers that follow a uniform distribution in the [0,1] interval, serving to increase the randomness of particle search.

## 5.1 Basics of PSO

The IA is an algorithm inspired by biological immune systems. As shown in Table 1, it is similar to the human body's defense mechanism, possessing abilities similar to immune memory and self-regulation, and demonstrating advantages in diversity and global optimization [18-20].

**Table 1** Analogy of immune system and immune algorithm

| Immune system | Immune algorithm |
|---|---|
| Antigen | Problem to be optimized |
| Antibody | Feasible solution to the problem |
| Affinity | Quality of feasible solutions |
| Cellular activation | Immune selection |
| Cell differentiation | Individual cloning |
| Affinity maturation | Variation |
| Clone inhibition | Clone inhibition |
| Dynamically maintaining balance | Population refresh |

In IAs, affinity is used for the selection and assessment of antibodies, which include the affinity (matching degree) between antigens and antibodies, as well as the affinity (similarity degree) between antibodies. The main parameters of the Immune Algorithm are explained as follows:

(1) Affinity essentially reflects how tightly immune cells bind to specific antigens; a concept similar to the fitness concept in genetic algorithms. The function that assesses affinity, commonly referred to as *aff*(*x*), takes an instance of an antibody in the $S \in \boldsymbol{R}$ interval as input (where S represents the set of feasible solutions and $\boldsymbol{R}$ represents the range of real numbers), and outputs the corresponding affinity value. For standard function optimization problems, function values or their transformations (such as reciprocals) can be directly used as affinity. For more complex composite or application-level problems, the evaluation methods should be refined according to specific circumstances.

(2) Antibody Concentration Antibody concentration is an indicator of population diversity. If it is too high, it indicates a large number of highly similar individuals are concentrated in a specific area of the solution space, which is not conducive to maintaining the global search capability of the algorithm. To avoid this concentration phenomenon, the algorithm should suppress individuals with high concentration to ensure population diversity.

$$\text{den}(ab_i) = \frac{1}{N}\sum_{j=1}^{N} S(ab_i, ab_j) \tag{31}$$

$$S(ab_i, ab_j) = \begin{cases} 1, & aff(ab_i, ab_j) < \delta_s \\ 0, & aff(ab_i, ab_j) \geq \delta_s \end{cases} \quad (32)$$

where $N$ is the population size, den($ab_i$) denotes the concentration of the antibody, $S(ab_i,ab_j)$ represents the similarity between antibody $i$ and antibody $j$, $\delta_s$ is the similarity threshold.

Generally speaking, antibody concentration is inversely defined, which means a lower concentration implies a higher value. Accordingly, a clear definition of the affinity between antibodies is a critical prerequisite for concentration evaluation. The commonly mentioned affinity of antigens to antibodies also applies to the concept of affinity used for measuring the similarity between two antibodies. Common methods for calculating the affinity between antibodies include, but are not limited to, affinity-based methods, Euclidean distance, Hamming distance, and informational entropy. The appropriate method should be chosen based on the actual problem at hand.

(3) Stimulatory Degree. The stimulatory degree plays a decisive role in assessing the quality of an antibody, making a comprehensive judgment based on the antibody's affinity as well as its concentration. In most cases, antibodies that combine high affinity (reflected in superior objective function values) with low concentration tend to have relatively high stimulatory degrees (i.e., superior performance). The stimulatory degree is typically calculated by processing the results of antibody affinity and concentration assessments in a straightforward manner.

$$\text{sim}(ab_i) = a \cdot aff(ab_i) - b \cdot \text{den}(ab_i) \quad (33)$$

where sim($ab_i$) is the stimulation intensity of the antibody $i$, with $a$ and $b$ being the computation parameters.

## 5.2 Principle of IPSOA

The PSO and IA are both heuristic algorithms used for problem-solving that draw inspiration from the dynamic changes in biological characteristics found in nature. Despite their similarities, they also exhibit distinct differences. PSO improves the search for solutions through the coordinated cooperation among particles within the swarm, constantly adjusting their paths to seek local and global optima within the solution space. In contrast, IAs mimic the mechanisms that generate antibodies within the biological immune system—continuously producing and selecting new antibodies to find the optimal solution.

PSO focuses on the synergistic effect of information exchange between individuals and the group, adjusting particles' positions and velocities within the solution space to enhance diversity. On the other hand, IAs maintain diversity within the antibody population through mechanisms such as immune memory, concentration regulation, and vaccination [21]. The PSO emphasizes mutual assistance among particles, with iterations depending on the incorporation of personal and group cognition into each particle's position and velocity changes. IAs rely on selection, crossover, and mutation for antibody iteration updates, introducing more random elements.

However, a single strategy often fails to yield the best results due to inherent limitations. The PSO allows particles to evolve through cooperation, but if particles become too concentrated in a specific area, diversity decreases, making it easy to fall into local optima and converge prematurely. IAs use memory and concentration regulation mechanisms to maintain diversity and introduce vaccination to prevent premature elimination of high-quality particles, but they tend to have weaker inter-antibody cooperation and underutilize feedback information, possibly leading to redundant iterations and decreased efficiency and accuracy.

Given the strengths and weaknesses of both methods, an integrated strategy, the IPSO, has been developed [22] In this strategy, the special mechanisms of IAs are integrated into the PSO framework. The optimization process involves selection and the generation of new particles—now considered antibodies [23]. Using an immune memory bank to store excellent particles and adopting an elitism strategy to select and preserve them, this prevents high-fitness particles from being eliminated due to decreased concentration. An immune concentration selection ratio formula is used to determine each particle's probability of being chosen, based on which dominant particles are added to the immune memory while suboptimal particles are eliminated. Vaccination ensures the continued diversity of the population in the later stages of the algorithm, further improving the efficiency and precision of the PSO's problem-solving capabilities [24].

During the application process of the IPSOA, the first step is to estimate the concentration of antibodies and antigens of the particles within the system, then, based on the mathematical expressions of the particle concentrations within the system, probabilities for the existence of each particle are defined, and particles with overly high concentrations are eliminated according to these probabilities, with the aim of maintaining diversity among the particles [25]. Through algorithmic processing, mutant particles are created and replace those with initially high concentrations. The concentration of the $i$-th particle in the system is obtained through the following calculation formula:

$$D(x_i) = \frac{1}{\sum_{i=1}^{N+M} |f(x_i) - f(x_j)|} \quad (34)$$

The probability formula for the proportion of the quantity of the $i$-th individual to the total quantity of individuals

is as follows:

$$P(x_i)=\frac{\frac{1}{D(x_i)}}{\sum_{i=1}^{N+M}\frac{1}{D(x_i)}}=\frac{\sum_{j=1}^{N+M}|f(x_i)-f(x_j)|}{\sum_{i=1}^{N+M}\sum_{j=1}^{N+M}|f(x_i)-f(x_j)|} \tag{35}$$

As can be inferred from the abovementioned formula, the greater the concentration of particles, the lesser the chance they have of being selected, the converse is also true. Therefore, the distribution of particles in the solution space becomes more uniform, which reduces the problem of excessive particle concentration in certain areas and avoids limited searching, which is a predicament that PSO algorithms often face-premature convergence has been mitigated to some degree.

In summary, the IPSOA combines the advantages of PSO, such as group cooperation, information feedback, and rapid convergence, with the features of immune algorithms like memory functions, concentration adjustment, and a rich variety of antibodies. This strategy effectively prevents the potential issue of premature convergence during the later stages of iterative processes, significantly enhancing the algorithm's efficiency and accuracy of solutions in its latter phases.

### 5.3 IPSOA for location and capacity determination of EV charging stations

(1) Input the original parameters, which include data related to "Vehicle-Road-Power": road network matrix model $G$, power grid matrix model $P$, the number of EVs $N$, the spatiotemporal distribution matrix of EV charging load $M$, EV user charging cost. Data relevant to the IPSOA: maximum number of iterations $K_{max}$, particle population size $N$, particle population dimension $n$, maximum weight, minimum weight, learning factors $c_1$, $c_2$. Set the population size, solving precision, mutation probability, etc.

(2) Set the number of candidates charging stations $N_s$ and the set of candidate locations $D_s$. The candidate locations for charging stations are based on the division of urban functional zones, that is, the geometric center coordinates of each functional zone within the research area are used as the candidate locations. The candidate location set $D_s$ determines the matrix dimension based on the particle population size parameter from the IPSOA in (1).

(3) Based on Eq. (6)-(19), the total societal cost $C$ of the planned charging station is calculated by integrating the operational cost $C_{op}$ of the EV charging station, the EV user's charging cost $C_u$, and the power grid loss cost $C_p$. The charging station location coordinates are preliminarily selected with the objective function being the minimization of the total social cost $C$. Based on Eq. (20)-(27), which integrate constraints from the charging station operators, users, and power distribution network, particle positions that do not meet the constraints are eliminated, and the retained charging station locations enter the candidate location set $D_s$.

(4) Calculate the total social cost $C$ as the particle fitness, update and iterate particle velocities and positions based on the movement speed and position of immune particles, and record individual and global extremes.

(5) Update the global extremum. Compare individual extremes within the current particle swarm $A_k$ with the global extreme $P_{k\,g}$, and update the extremum.

(6) Determine if the iteration should terminate. If the current number of iterations $k$ has exceeded the maximum allowed value $K_{max}$, stop iteration, and consider the fitness value of the obtained global extremum as the best solution of, if not yet at the termination point, proceed to (7).

(7) Generate new particles. Applying the principle of vaccine inoculation from the immune particle swarm, generate $M$ new particles to update individual extremes ($i$=$N$+1, $N$+2, …, $N$+$M$) and the global extremum $P_g$ of the particle swarm. Calculate the selection probability $P(x_i)$ simultaneously.

(8) Construction and update of the memory bank. According to the selection strategy, prioritize the top $S$ particles with the highest fitness in the particle swarm to store in the memory bank. Thereafter, select $K$-$S$ high-quality particles from the remaining $N$+$M$-$S$ particles based on the selection probability for storage. Consequently, form the parental generation by choosing $N$ high-quality particles to form the particle swarm $B_k$. Update particle information afterwards, according to Eq. (30), update the new particle swarm $B_k$'s velocity, position, fitness, and individual extremums.

(9) Fusion of particle swarms. Combine $K$ excellent particles from the memory bank with the existing particle swarm, and remove the $K$ particles with relatively lower fitness to form a new round of particle swarm $A_k$ with a scale of $N$. Continue to return to (5) until the fitness stabilizes and ultimately output the charging station siting scheme with the minimum social cost.

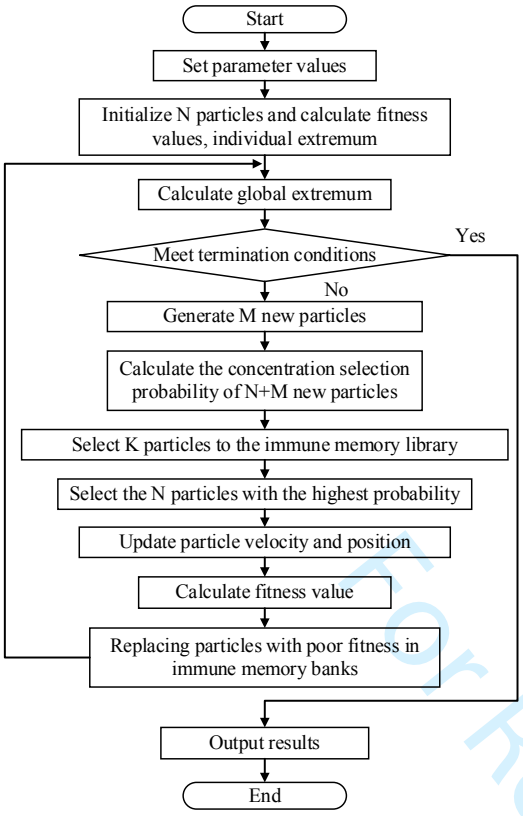


**Fig. 5. Flow chart of immune particle swarm optimization**

### 5.4 IPSOA test

To verify the efficient convergence characteristics of the new algorithm that embody both immune and particle swarm strategies, as well as the ability of particles to accelerate breakthroughs when trapped near local optima, this paper selects two common test functions: the Sphere function and the Rastrigin function. These two functions represent typical unimodal and multimodal problems, respectively, and the minimization objective value for both functions is 0. The basic formulas and parameters of the two functions are shown in Table 2.

**Table 2** Basic test function parameters table

| | Function | Test type | Value | Search space dimension |
|---|---|---|---|---|
| $f_{test1}$ | Sphere function | Unimodal testing | [-10,10] | 10 |
| $f_{test2}$ | Generalized-Rastrigin | Multimodal testing | [-5,5] | 5 |

$$f_{test1}(x)=\sum_{i=1}^{n}x_i^2 \tag{36}$$

$$f_{test2}(x)=\sum_{i=1}^{n}\left[x_i^2-10\cos(2\pi x_i)+10\right] \tag{37}$$

The parameter settings for each algorithm are as follows: in the PSO algorithm, $\omega$ is set to 0.9, $c_1$ is set to 0.5, and $c_2$ is set to 0.7, in the IPSOA, $\omega_{max}$ is set to 0.9, $\omega_{min}$ is set to 0.5, with a cloning mutation probability, additional particles $M$=10, and a memory bank capacity $K$=4. The particle population size for both algorithms is 20, and the maximum number of iterations is set to 100. MATLAB was used to encode and simulate the algorithms, resulting in the outcomes as illustrated in the figures.

The two algorithms were implemented to find the optimal solutions for two distinct functions, using MATLAB software for ten runs each, yielding the comparative experimental data results displayed in Table 3.

An analysis of the fitness function iteration curves displayed from Figures 6 to 7, along with the experimental data in Table 3, reveals the following findings: The Immune Particle Swarm Optimization (IMPSO) algorithm is capable of

maintaining a high diversity of particles in the latter stages of iteration, which in turn enhances the efficiency and accuracy of the global optimal solution search. For unimodal function problems, both PSO and IMPSO are able to rapidly converge to the global best solution, however, when dealing with more complex multimodal problems, traditional PSO (PSO) may lead to excessive particle convergence, limiting population diversity. The immune particle swarm algorithm enables particles to converge more quickly to the vicinity of the global best solution and performs effective searches within this area, thus significantly outperforming the standard PSO in terms of speed and accuracy. The Immune Particle Swarm method calculates the selection probability based on particle similarity assessment and selects high-quality particles from the population for memory bank storage according to this probability. It also adopts an elite reservation mechanism to prevent the abandonment of high-fitness particles, ensuring that population diversity is maintained in the late stages of iteration and avoiding the risk of losing dominant particles due to premature convergence.

**Table 3** Basic Test Function Solution Results

| Frequency | $f_{test1}$ | | $f_{test2}$ | |
|---|---|---|---|---|
| | PSO | IA-PSO | PSO | IA-PSO |
| 1 | 0.172 | 0.000665 | PSO | IA-PSO |
| 2 | 0.0768 | 0.00518 | 0.00466 | 5.19E-6 |
| 3 | 0.124 | 0.000199 | 0.0232 | 7.92E-5 |
| 4 | 0.0345 | 0.000298 | 0.00497 | 4.78E-5 |
| 5 | 0.0618 | 0.00581 | 0.00191 | 2.83E-5 |
| 6 | 0.0866 | 0.00673 | 0.0245 | 9.76E-6 |
| 7 | 0.492 | 0.000845 | 0.00593 | 8.34E-5 |
| 8 | 0.0422 | 0.000683 | 0.0686 | 7.45E-7 |
| 9 | 0.00352 | 0.00793 | 0.0427 | 8.74E-5 |
| 10 | 0.829 | 0.000945 | 0.00746 | 9.47E-7 |

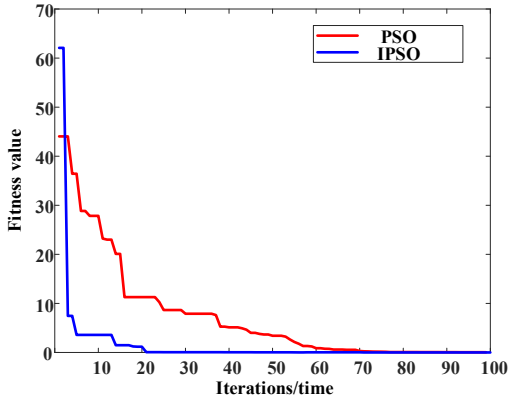


**Fig. 6. Test function $f_{test1}$ fitness iteration curve**

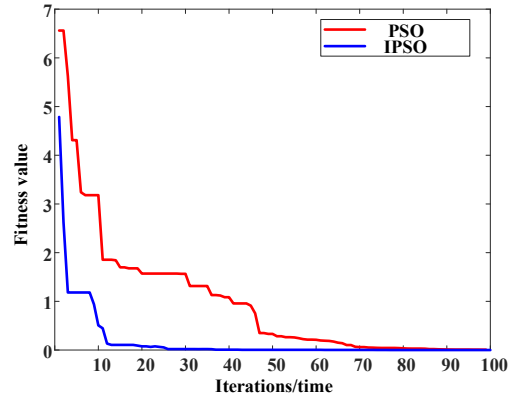


**Fig. 7. Test function $f_{test2}$ fitness iteration curve**

## 6 Case study and results analysis

### 6.1 Example parameters

Employing the road network structure with a 33-node distribution grid as the subject of study, the distribution capacity is to be adjusted reasonably. The correspondence between the road network nodes and the electrical grid nodes is shown in Table 4. It is important to note that the road network nodes do not have a one-to-one correspondence with the electrical grid nodes, rather, a single node in the distribution system can supply power to an entire area, and road network nodes are situated within these regions, thus establishing their correlation. The planning of charging stations within the study area is conducted using the forecasted results of the spatiotemporal distribution of charging demand as input for the charging station planning model, which serves to validate the feasibility of the model established in this paper. The settings for the model's related parameters are presented in Table 5. The functional area division and charging load in the calculation example are based on the data from [26].

**Table 4** Corresponding relationship between road network and grid nodes

| RNNs | GNs | RNNs | GNs | RNNs | GNs |
|---|---|---|---|---|---|
| 22 | 1 | 238 | 12 | 13 | 23 |
| 62 | 2 | 222 | 13 | 6 | 24 |
| 48 | 3 | 190 | 14 | 17 | 25 |
| 94 | 4 | 136 | 15 | 145 | 26 |
| 147 | 5 | 120 | 16 | 69 | 27 |
| 178 | 6 | 32 | 17 | 35 | 28 |
| 170 | 7 | 14 | 18 | 31 | 29 |
| 192 | 8 | 133 | 19 | 85 | 30 |
| 196 | 9 | 183 | 20 | 79 | 31 |
| 224 | 10 | 200 | 21 | 124 | 32 |
| 246 | 11 | 241 | 22 | 75 | 33 |

**Table 5** Simulation parameter settings

| Parameter | Numerical value |
|---|---|
| $C_{opcp}$ | 5000 CNY |
| $C_{opce}$ | 10000 CNY |
| $C_{oprp}$ | 10000 CNY |
| $C_{ep}$ | 0.8 CNY/kWh |
| $C_t$ | 20 CNY/h |
| $C_{chp}$ | 1 CNY/kWh |
| $C_{lossp}$ | 0.5 CNY/kWh |
| m (service life of charging station) | 20 years |
| $W_{qmax}$ | 0.5h |
| EV range | 300km |
| EV battery capacity | 20kWh |
| Maximum investment amount | 20 million CNY |
| α | $20m^2$ |
| $l_S$ | 5km |
| Copcb | 250000 CNY |
| $t_r$ | 7300h |
| $C_{rs}$ | 2000 CNY/$m^2$ |
| $C_{rh}$ | 1500 CNY/$m^2$ |
| $C_{rw}$ | 800 CNY/$m^2$ |
| $C_{r0}$ | 50000 CNY/$m^2$ |
| $r_0$ | 2% |
| $P$ | 5kW |
| $N$ | 100 |
| $K_{max}$ | 200 |
| $n$ | 4 |
| Maximum weight | 1.5 |
| Minimum weight | 1.9 |
| Learning factor $c_1$ | 0.5 |
| Learning factor $c_2$ | 0.5 |
| Solution accuracy | 0.001 |
| Mutation probability | 3% |

**Table 6** Number of charging stations and corresponding social costs (in 10000 CNY)

| Charging stations No. | $C_{op}$ | $C_u$ | $C_p$ | $C_{min}$ |
|---|---|---|---|---|
| 7 | 874.7 | 736.7 | 90.5 | 1701.9 |
| 8 | 885.3 | 694.3 | 115.9 | 1695.5 |
| 9 | 911.4 | 582.1 | 167.6 | 1661.1 |
| 10 | 928.4 | 544.3 | 230.4 | 1703.1 |
| 11 | 963.5 | 510.4 | 269.3 | 1743.2 |
| 12 | 986.3 | 448.2 | 322.4 | 1756.9 |
| 13 | 1017.5 | 437.9 | 352.9 | 1808.3 |

## 6.2 Analysis of siting and sizing results

(1) Impact of charging station number on total social cost

By analyzing the impact of the number of charging stations on total societal cost, one can determine the minimal number of charging stations resulting in the lowest societal cost. The relationship between the number of charging stations and total societal cost is depicted in Figure 8, and the correlation between the number of charging stations and respective societal costs is demonstrated in Table 6.

When planning the number of charging stations, it is found that having fewer than 7 or more than 15 stations cannot meet the constraint conditions. As shown in the figure, when the number of planned, charging stations is set to 9, the minimum total social cost is achieved. It can be seen from the table that, with the increase in the number of charging stations, the cost to operators for charging facilities and maintenance increases, and the cost of power grid losses also goes up. However, at the same time, user costs decrease significantly due to reduced travel time to the stations and shorter queuing times. Therefore, the optimal number of charging stations that balances the costs for operators, the EV users' charging costs, and the power grid loss is 9.

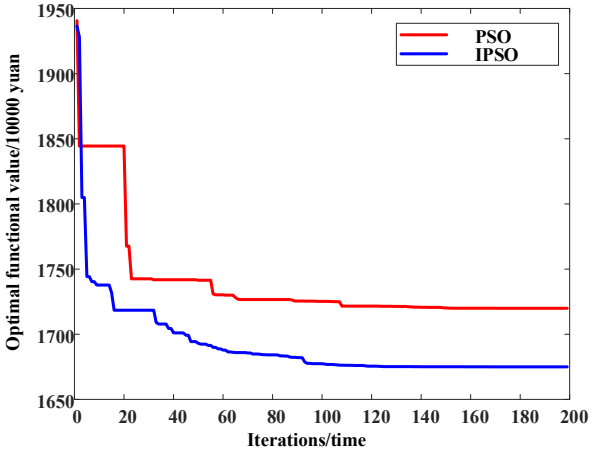


**Fig. 9. Comparison of PSO algorithm and IPSOA iterations**

(2) Iteration comparison between PSO and IPSO

Figure 9 illustrates the iterative comparison between PSO and IPSOAs. Analysis of Figure 9 shows that the convergence speed of the immune particle swarm algorithm is significantly higher than that of the standard PSO. The PSO converges around the 149th generation with an optimal result of approximately 17.3 million Yuan, while the immune particle swarm algorithm converges around the 94th generation with an even lower social total cost of about 16.7 million Yuan.

(3) The siting and sizing results under different schemes.

To verify the effectiveness of the simulation method, three schemes are proposed for comparison: Scheme 1: prioritizes the lowest operational costs for EV charging station operators, Scheme 2: prioritizes the lowest charging costs for EV users, and Scheme 3: comprehensively considers and minimizes the costs for EV charging stations operators, users' charging costs, and power grid loss costs. The simulation results for these three schemes are shown in Table 7, while the costs are illustrated in Figure 10.

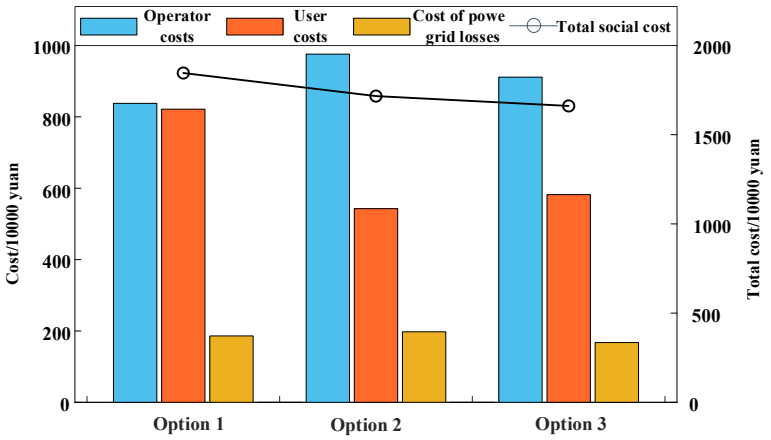


**Fig. 10. Cost comparison of three charging station site selection and capacity determination schemes**

**Table 7** Results of IPSOA for site selection and capacity determination of charging stations

| Option | No. | Coordinates | Functional zone | Allocation |
|---|---|---|---|---|
| O_1 | 1 | (11542360.781,4317111.715) | PSA | 21 |
| | 2 | (11540574.840,4316463.484) | PSA | 24 |
| | 3 | (11544596.514,4316714.839) | PSA | 26 |
| | 4 | (11542188.801,4315312.544) | PSA | 20 |
| | 5 | (11544173.180,4313328.165) | WA | 18 |
| | 6 | (11545932.663,4313883.791) | WA | 21 |
| | 7 | (11547162.978,4313711.812) | PSA | 23 |
| | 8 | (11542162.343,4318090.675) | WA | 17 |
| | 9 | (11548380.063,4314095.459) | PSA | 23 |
| O_2 | 1 | (11541950.676,4317892.237) | R1A | 27 |
| | 2 | (11541381.820,4316675.151) | R1A | 24 |
| | 3 | (11541831.613,4315722.649) | R1A | 24 |
| | 4 | (11542982.553,4314293.896) | CD | 26 |
| | 5 | (11544966.932,4316516.401) | R1A | 17 |
| | 6 | (11545416.724,4314704.001) | PSA | 25 |
| | 7 | (11547731.833,4315286.086) | PSA | 25 |
| | 8 | (11548049.334,4313897.021) | R1A | 23 |
| | 9 | (11546157.559,4314492.334) | CD | 14 |
| O_3 | 1 | (11541791.925,4316886.818) | WA | 18 |
| | 2 | (11541196.612,4315854.941) | R1A | 21 |
| | 3 | (11543207.449,4313844.104) | R1A | 20 |
| | 4 | (11544530.368,4313685.354) | CD | 25 |
| | 5 | (11543591.096,4315312.544) | R1A | 23 |
| | 6 | (11543352.970,4317072.027) | CD | 15 |
| | 7 | (11547586.312,4314042.542) | PSA | 28 |
| | 8 | (11546355.997,4314915.669) | PSA | 27 |
| | 9 | (11544781.723,4316053.379) | WA | 22 |

According to Table 7, Scheme 1 has charging stations primarily situated in public service areas and work areas, Scheme 2 locates more stations in residential areas, while the placement of charging stations in Scheme 3 does not show clear similarity in the functions of their respective areas. The primary reason for these differences lies in the distinct optimization objectives of each scheme. Scheme 1 prioritizes the lowest operational costs for EV charging station operators, which are mainly influenced by the acquisition cost of charging facilities, maintenance costs, and site leasing fees. Therefore, this scheme tends to choose locations in areas where rents are relatively low and has the fewest number of charging piles.

Furthermore, as known from Table 8, although Scheme 1 has the lowest operational costs for operators, it results in increased travel and queuing costs for users, making the user cost the highest among the three schemes. Scheme 2 gives priority to minimizing the charging costs for EV users, thereby tending to concentrate charging stations in densely populated residential areas to facilitate user convenience. However, this also leads to increased operational costs for operators. Scheme 3 comprehensively considers the lowest costs for EV charging station operators, users' charging

costs, and power grid loss costs. Under this scheme, both the power grid loss and the total societal costs are the lowest. The locations for Scheme 3 are illustrated in Figure 11.

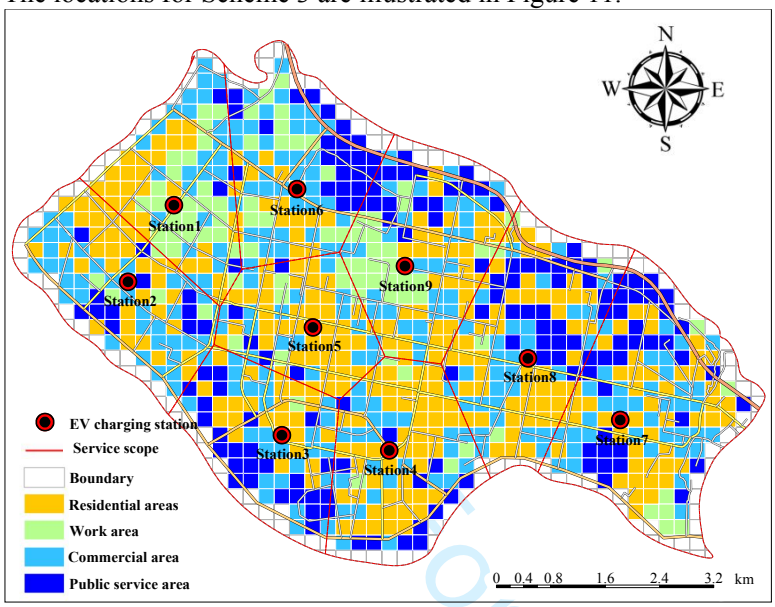


**Fig. 11. IPSOA for charging station site selection and capacity determination results**

**Table 8** Cost Comparison of Three Charging Station Site Selection and Capacity Determination Results (in 10000 CNY)

| Option | $C_{op}$ | $C_u$ | $C_p$ | $C_{min}$ |
|---|---|---|---|---|
| 1 | 837.9 | 821.6 | 186.3 | 1845.8 |
| 2 | 975.7 | 542.9 | 197.8 | 1716.4 |
| 3 | 911.4 | 582.1 | 167.6 | 1661.1 |

An analysis of Figure 11 indicates that Station 7 has the largest service area, encompassing many residential zones with concentrated charging demands, which explains why it has the highest number of charging piles. Stations 8, 4, and 5 have a service range that includes a moderate amount of residential areas. Station 6's service range encompasses numerous work, commercial, and public service areas, where the charging demand is more dispersed, which is why it has the fewest number of charging piles.

## 7 Conclusions

This paper proposes an urban EV charging station location and capacity optimization model that takes into account the comprehensive interests of "vehicle-station-network" Based on the simulation experiment of the algorithm example, the following conclusions can be drawn:

(1) The proposed IPSOA has good convergence properties and is particularly advantageous when solving multi-objective functions.

(2) There is a nonlinear relationship between the number of charging stations and the total social cost. The lowest total social cost is achieved when the number of charging stations is set to 9.

(3) The proposed method takes into account the interests of charging station users, operators, and electric power networks. Compared with the other two siting schemes, it has reduced the operator cost and user cost, as well as the power grid loss cost. The power grid loss cost is reduced by 11.1% and 17.8%, respectively, and the total societal cost is reduced by 9.96% and 3.22%, respectively.

In this paper, an urban EV charging station location and capacity optimization model considering the comprehensive interests of "vehicle-station-network" is used to simulate the siting and sizing of charging stations within the study area. The proposed algorithm conforms to the actual situation and has certain reference value. However, with the rapid development of 5G communication, the coalescence of multi-source information within the urban smart transportation system will become more intricate. This will also provide a more diverse data source for the siting and

sizing of EV charging stations. Exploring the interactive relationships among these factors and proposing more efficient siting methods will be a hot topic for future research.

## References


[1] Y. Feng, X. Zhao, G. Ren, et al., "Planning method for urban centralized charging stations," Journal of Power Systems and Automation, vol. 30, no. 8, pp. 58-61+67, Aug. 2018. (in Chinese)

[2] L. Jia, Z. Hu and Y. Song, "Comprehensive planning of urban electric vehicle charging facilities considering different types of charging needs" Grid Technology, vol. 40, no. 9, pp. 2579-2587, Sept. 2016.

[3] S. Ge et al., "Charging station planning considering traffic flow information and distribution network capacity constraints," Grid Technology, vol. 37, no. 3, pp. 582-589, Jan. 2013.

[4] W. Huang, "Research on electric vehicle charging load prediction and charging station location and capacity determination," Nanjing: Nanjing University of Posts and Telecommunications, Oct ,2023.

[5] D. Guo et al., "Layout planning method for emergency charging facilities of electric vehicles," Power System Automation, vol. 47, no. 16, pp. 66-75, Jun. 2023.

[6] Q. Xu et al., "Electric vehicle charging station site planning considering driver behavior habits and travel chain," Power System Automation, vol. 40, no. 4, pp. 59-65+77, Feb. 2016.

[7] S. Peng, H. Zhang, Y. Yang, et al., "Spatial-temporal dynamic forecasting of EVs charging load based on DCC-2D," Chinese Journal of Electrical Engineering, 2022, 8(1): 53-62.

[8] F. Wu, and R. Sioshansi, "A stochastic flow-capturing model to optimize the location of fast-charging stations with uncertain electric vehicle flows," Transportation Research Part D: Transport and Environment, vol. 53, pp. 354-376, Jun. 2017.

[9] M. Kchaou-Boujelben and C. Gicquel, "Locating electric vehicle charging stations underncertain battery energy status and power consumption," Computers & Industrial Engineering, vol. 149, pp. 747-752, Nov. 2020.

[10] O. Arslan and O. E. Karaan, "A benders decomposition approach for the charging station location problem with plug-in hybrid electric vehicles," Transportation Research Part BMethodological, vol. 93, pp. 670-695, Nov. 2016.

[11] C. Lee and J. Han, "Benders-and-price approach for electric vehicle charging station locationproblem under probabilistic travel range," Transportation Research Part BMethodological, vol. 106, pp. 130-152, Dec. 2017.

[12] J. Hondgsonm, "A flow capturing location allocation model," Geographical Analysis, Jul.1990

[13] H. Wang et al., "Planning of electric vehicle charging stations considering traffic network flow," Power System Automation, vol. 37, no. 13, pp. 63-69+98, Apr. 2013.

[14] W. Yao et al., "Coordinated planning of distribution system and electric vehicle charging network," Power System Automation, vol. 39, no. 9, pp. 10-18, May. 2015.

[15] X. Huang et al., "Optimization planning of electric vehicle charging stations based on LCC and quantum genetic algorithm," Power System Automation, vol. 39, no. 17, pp. 176-182, Sept. 2015.

[16] J. Lian et al., "Design and implementation of a 3D visualization system based on ArcScene," Geospatial Information, vol. 39, no. 1, pp. 83-86, Feb. 2008.

[17] L. Zhang et al., "Solving multi-objective optimization problems based on particle swarm optimization algorithm," Computer Research and Development, vol. 37, no. 7, pp. 1286-1291, Jul. 2004.

[18] L. Wang, J. Pan and L. Jiao, "Immune algorithm," Journal of Electronics, vol. 23, no. 7, pp. 74-78, Jul. 2000.

[19] J. Lin et al., "Reactive power optimization based on adaptive immune algorithm," International Journal of Emerging Electric Power Systems, vol. 10, no. 4, pp. 231-237, Jan. 2009.

[20] J. Yuan et al., "An immune-algorithm-based dead-time elimination PWM control strategy in a single-phase inverter," Power Electronics IEEE Transactions, vol. 30, no. 7, pp. 3964-3975, Aug. 2015.

[21] Q. Mei, "Research on cold chain logistics distribution path optimization based on immune particle swarm optimization algorithm," Xi'an: Xi'an University of Electronic Science and Technology, Jun. 2020.

[22] Y. Gao, and S. Xie, "Immune particle swarm optimization algorithm," Computer Engineering and Applications, vol. 25, no. 6, pp. 4-6+33, Feb. 2004.

[23] B. Yang, "Dynamic risk identification safety model based on fuzzy support vector machine and immune optimization algorithm," Safety Science, vol. 118, pp. 205-211, Oct. 2019.
[24] X. Xue, "Evaluation of concrete compressive strength based on an improved PSO-LSSVM model," Computers & Concrete, vol. 21, no. 5, pp. 505-511, May. 2018.
[25] C. Zhang et al., "Immune particle swarm optimization algorithm based on adaptive search," Journal of Engineering Science, vol. 39, no. 1, pp. 125-132, Jan. 2017.
[26] H. Li, Y. Song, S. Li, et al., "Electric vehicle charging load prediction based on ArcGIS road network structure and traffic congestion analysis," Power System Technology, pp. 1-14, 2023, doi: 10.13335/j.1000-3673.pst.2023.1420.